Supplementary Information (SI) for Physical Chemistry Chemical Physics.
This journal is © the Owner Societies 2024

Supplementary Material

Diffusional and thermodynamics properties of lithium polysulfides in different solvents: a Molecular Dynamics approach

Javier Luque Di Salvo[1*], Santiago Agustín Maldonado-Ochoa[2,3], Guillermina L. Luque[1], Andrea Calderón[2], Victoria Bracamonte[2], Fabián Vaca Chávez[2,3], Daniel E. Barraco[2,3], Alen Vizintin[4], Robert Dominko[4,5], Ezequiel P. M. Leiva[1*], Giorgio De Luca[6]

[1] *Departamento de Química Teórica y Computacional, INFIQC, Av Medina Allende y Haya de la Torre, Ciudad Universitaria, CP X5000HUA Córdoba, Argentina.*

[2] *CONICET, Instituto de Física Enrique Gaviola (IFEG), Córdoba, Argentina.*

[3] *Universidad Nacional de Córdoba, Facultad de Matemática, Astronomía, Física y Computación, Córdoba, Argentina*

[4] *National Institute of Chemistry, Hajdrihova 19, SI-1000, Ljubljana, Slovenia*

[5] *ALISTORE-European Research Institute, CNRS FR 3104, Hub de l'Energie, Rue Baudelocque, 80039, Amiens Cedex, France*

[6] *Institute on Membrane Technology, ITM-CNR, Via P. Bucci 17/C, 87036, Rende (CS), Italy*

* *Corresponding Authors: javier.luquedisalvo@unc.edu.ar; ezequiel.leiva@unc.edu.ar*

Table S1. Solvent properties considered in the study.

Solvent	Chemical Formula	Donor Number (DN)	Static dielectric constant (ε_0)	Viscosity (η)[1]	Refractive Index
DMSO (dimethyl sulfoxide)	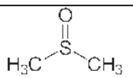	29.8	46.7	2	1.4793
DME (1,2-dimethoxyethane)	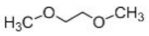	20	7.2	0.43	1.3781
ACN (acetonitrile)	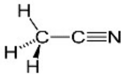	14.1	37.5	0.38	1.3441
DMF (N,N-dimethylformamide)	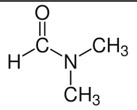	26.6	36.7	0.79	1.4305
DOL (1,3-dioxolane)	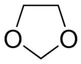	18	7.1	0.53	1.3992
TMS (sulfolane)	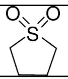	14.8	44	10.3	1.43025
DMA (N,N-dimethylacetamide)	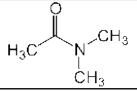	27.8	37.8	0.945	1.4375
TEGDME (tetraethylene glycol dimethyl ether)	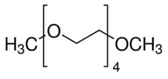	16.6	7.62	3.294	1.4841
DIOX (1,4-dioxane)	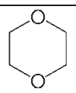	14.8	2.25	1.2	1.4224

[1] Viscosity units are centiPoise (cP)

The donor number of solvent mixtures is expected to be more similar to that of the pure solvent showing the highest DN[1]. However, since the exact form of the donor number for the mixtures considered in this study was not available, an arithmetic mean was used. In the case of DOL:DME mixture we used DN = 19 (expected to be closer to 20); in the case of DIOX:DME we adopted DN = 17.4 (expected to be closer to 20).

For the static dielectric constant, ε_0, of mixtures we employed the following expression[2]:

$$\varepsilon_0 = \varphi_A \varepsilon_{0,A}^{*} + \varphi_B \varepsilon_{0,B}^{*} \qquad \text{(Eq. S1)}$$

Here φ_A is the volume fraction of component A (similarly for component B), calculated as $\varphi_A = x_A V_A^{*}/\left(x_A V_A^{*} + x_B V_B^{*}\right)$, $x_A$and x_B being the molar fractions of A and B, V_A^{*} and V_B^{*} the partial molar volumes calculated as $V_A^{*} = m_A/\rho_A^0$ with m_A the molecular weight of A and ρ_A^0 the mass density of the pure liquid A. We note there is another option of interpolating between molecular polarizabilities which are better additives than partial molar volumes, but this choice has negligible effect on the resulting ionic partial charge.

For the viscosity, η, of solvent mixtures we employ the following expression[3,4]:

$$\eta = \eta_A^{*\,\varphi_A} \eta_B^{*\,\varphi_B} \qquad \text{(Eq. S2)}$$

The refractive index, n, was used to calculate the relative permittivity at high frequencies, ε_∞, which was used to scale the ion partial charges (electrostatic term of the force field) according to $q_{eff} = q/\sqrt{\varepsilon_\infty}$ as described in the main manuscript. For the mixtures, the following expression was employed[2]:

$$n = \sqrt{\varphi_A \left(n_A^{*}\right)^2 + \varphi_B \left(n_B^{*}\right)^2} \qquad \text{(Eq. S3)}$$

Table S2. Partial charges of terminal S (St), internal S (Si), and the resulting charge of S_6^{2-} (q_S6) and Li^+ (q_Li).

Solvent	St	Si	q_S6	q_Li
DOL:DME[5]	-0.4707	-0.1247	-1.4402	0.7201
ACN	-0.4863	-0.1288	-1.4880	0.7440
DIOX:DME	-0.4596	-0.1217	-1.4061	0.7030
DMA	-0.4547	-0.1204	-1.3913	0.6957
DME	-0.4743	-0.1256	-1.4513	0.7256
DMF	-0.4570	-0.1210	-1.3981	0.6991
DMSO	-0.4419	-0.1170	-1.3520	0.6760
TEGDME	-0.4405	-0.1166	-1.3476	0.6738
TMS	-0.4571	-0.1210	-1.3984	0.6992

Table S3. Composition of the simulation boxes used for the MSD computation, roughly yielding a concentration 0.05 M Li_2S_6.

Solvent	Number of Solvent Molecules	Number of Li^+ ions	Number of S_6^{2-} ions
ACN	7860	40	20
DME	3907	40	20
DIOX:DME	4321	40	20
DMSO	6218	40	20
DOL:DME	4677	40	20
DMA	4369	40	20
TEGDME	1898	40	20
TMS	4166	40	20
DMF	4809	40	20

Table S4. Composition of the simulation boxes used for the $\Delta G_{P,T}$ computation, roughly yielding a concentration 0.05 M Li_2S_6.

Solvent	Number of Solvent Molecules	Number of Li^+ ions	Number of S_6^{2-} ions
ACN	393	2	1
DME	195	2	1
DIOX:DME	216	2	1
DMSO	311	2	1
DOL:DME	234	2	1
DMA	218	2	1
TEGDME	95	2	1
TMS	208	2	1
DMF	240	2	1

The larger systems (Table S2) run 100 ns. The MSD curves were obtained by a time-ensemble average over 20 trajectories in the case of S_6^{2-} and 40 trajectories in the case of Li^+, the MSD curves are fitted in the range from 10 to 90 ns and the error reported in the self-diffusion coefficients is the "difference of the diffusion coefficients obtained from fits over the two halves of the fit interval" as default in the software[6], which works well for Brownian diffusion ($\beta \approx 1$ in Eq. 4).

For the smaller systems used to compute free energies (Table S3), we start with 2 Li^+ and 1 S_6^{2-} using a closed conformer structure[7] in the centre of the simulation box, then randomly inserting the corresponding number of solvent molecules. This procedure was repeated three times per solvent. Each of these systems was subjected to energy minimization by steepest descent, followed by 10 ns NPT which was checked as sufficient to obtain a well-equilibrated system. The last frame resulted from this simulation was used as a starting configuration to apply the λ-coupling (40 λ points). The standard deviation of the free energy values obtained in the three systems is the reported error in ΔG_{poly}^{solv} as well as in ΔH_{poly}^{solv}.

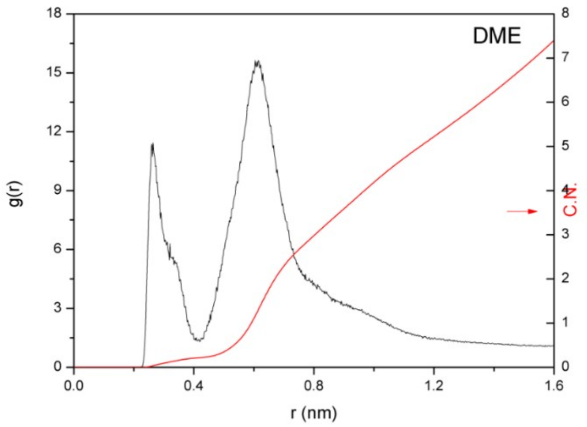
DME
g(r)
C.N.
r (nm)
0
3
6
9
12
15
18
0
1
2
3
4
5
6
7
8
0.0
0.4
0.8
1.2
1.6

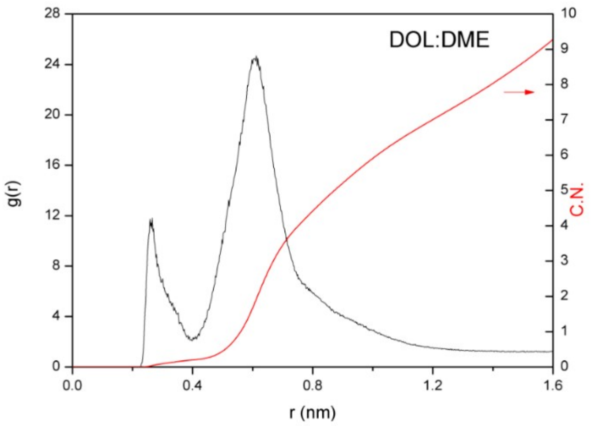
DOL:DME
g(r)
C.N.
r (nm)
0
4
8
12
16
20
24
28
0
1
2
3
4
5
6
7
8
9
10
0.0
0.4
0.8
1.2
1.6

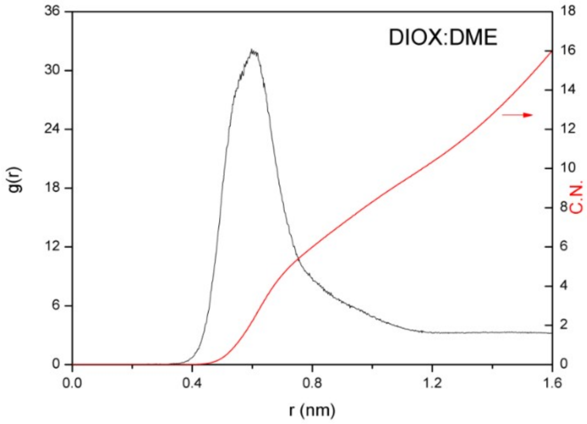
DIOX:DME
g(r)
C.N.
r (nm)
0
6
12
18
24
30
36
0
2
4
6
8
10
12
14
16
18
0.0
0.4
0.8
1.2
1.6

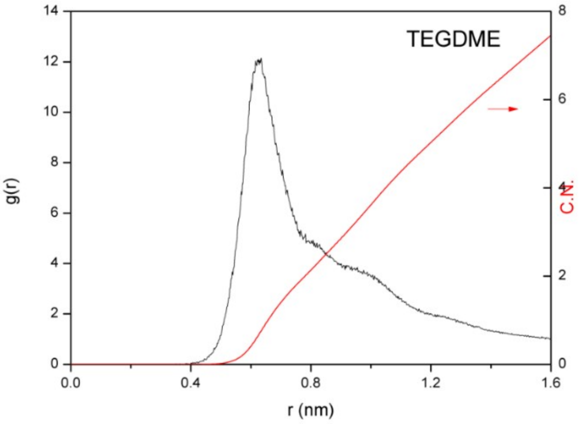
TEGDME
g(r)
C.N.
r (nm)
0
2
4
6
8
10
12
14
0
2
4
6
8
0.0
0.4
0.8
1.2
1.6

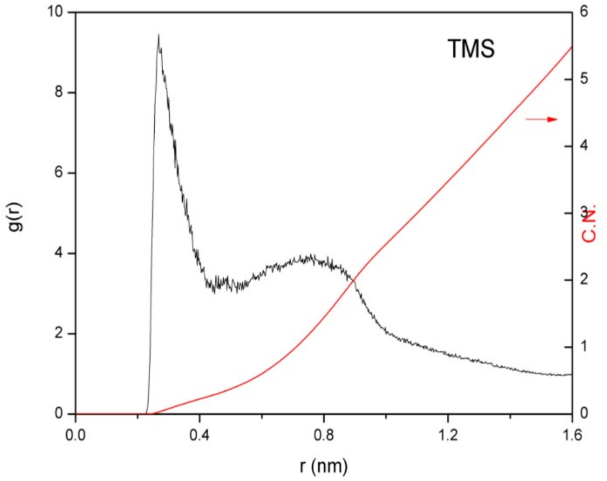
TMS
g(r)
C.N.
r (nm)
0
2
4
6
8
10
0
1
2
3
4
5
6
0.0
0.4
0.8
1.2
1.6

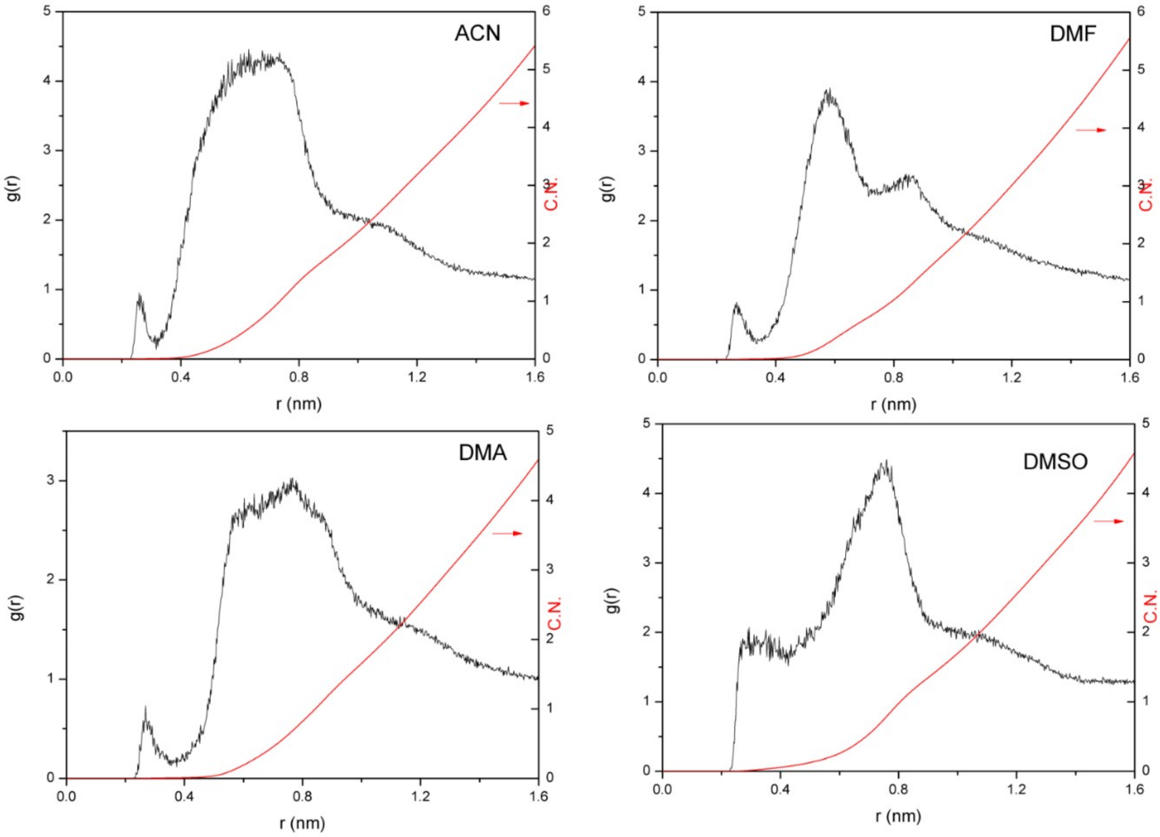

Figure S1. Radial distribution functions of Li-S, and the corresponding cumulative numbers (C.N.), for Li_2S_6 0.05M in different solvents.

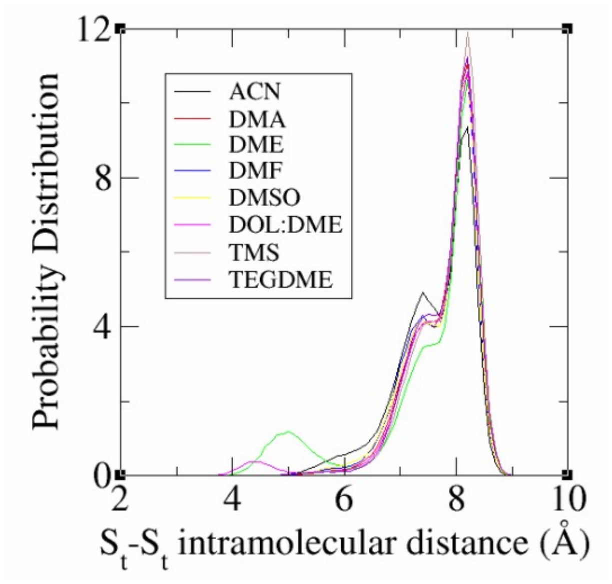

Figure S2. Probability distribution of hexasulfide conformation in Li_2S_6 0.05 M in different solvents, the S_t-S_t (terminal S atoms) intramolecular distance is used as descriptor. We have performed the same analysis as described in reference.[7]

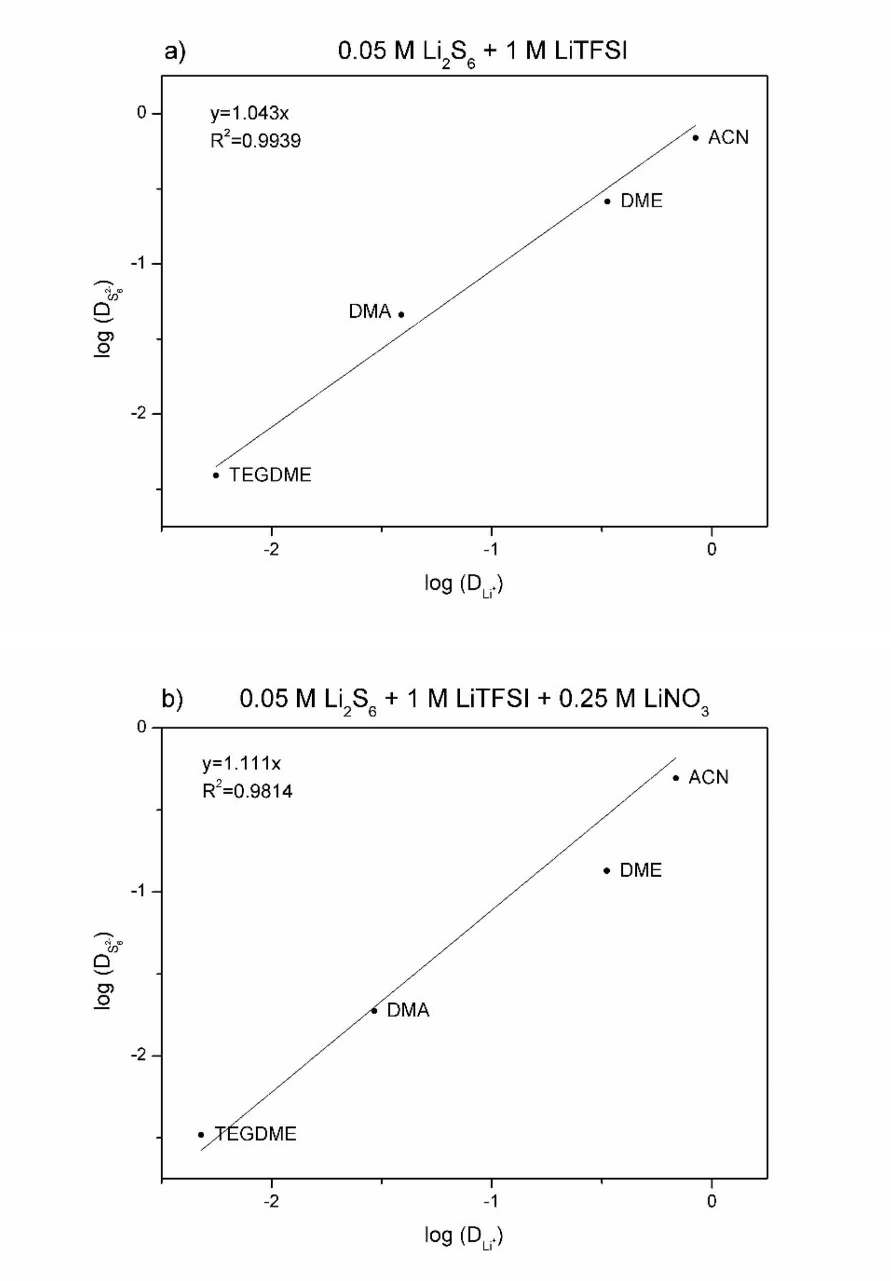

Figure S3. Correlation between $D_{S_6^{2-}}$ and D_{Li^+} for solutions of electrolytes containing different solvents. (a) 0.05 M Li_2S_6 + 1M LiTFSI, the linear fit yields a slope of 1.04 ± 0.07. (b) 0.05 M Li_2S_6 + 1M LiTFSI + 0.25 M $LiNO_3$, the linear fit yields a slope of 1.11 ± 0.08.

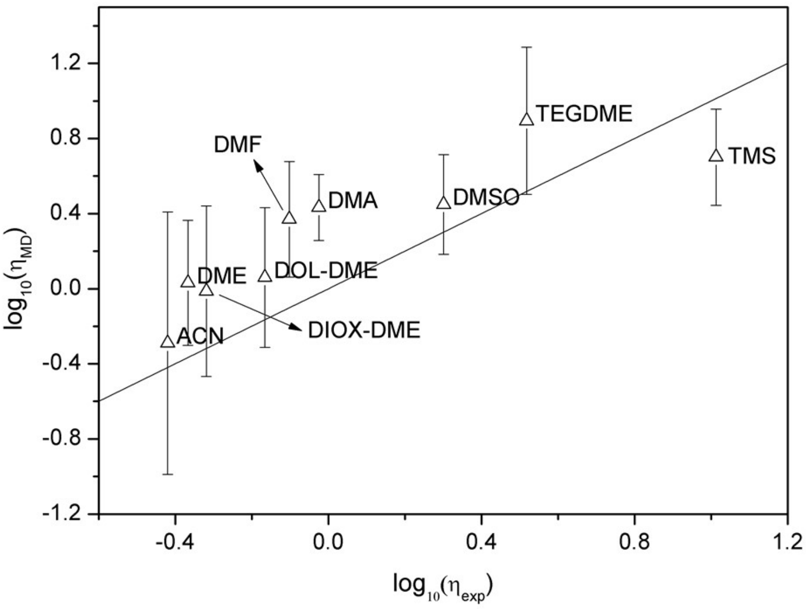

Figure S4. Comparison between computed (η_{MD}) and experimental viscosities (η_{exp}) in logarithmic scale. The straight line shows 1:1 correlation.

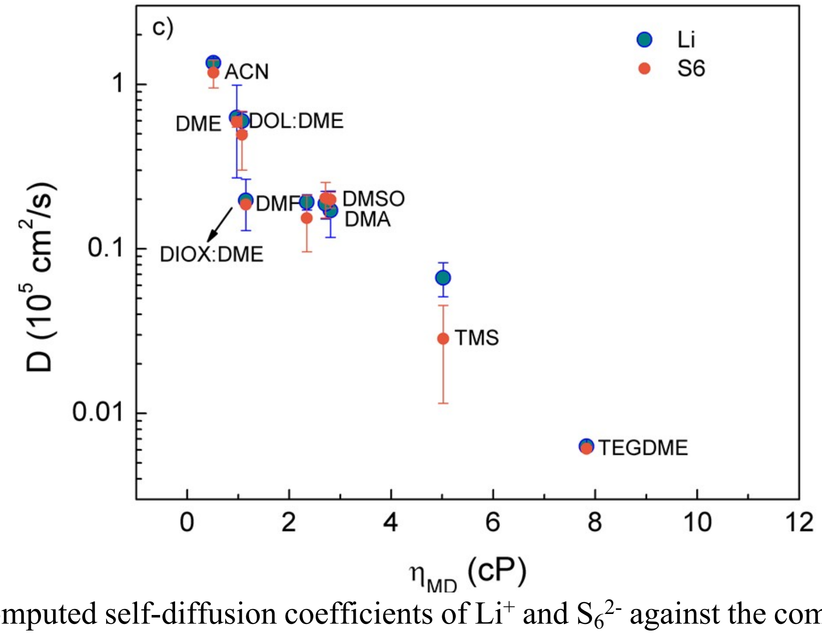

Figure S5. Computed self-diffusion coefficients of Li^+ and S_6^{2-} against the computed viscosity (cP).

Viscosities were calculated by the transverse current autocorrelation functions following the procedure reported elsewhere[8]. In detail, we run 100 ps from the last frame obtained from the 100 ns simulations, saving velocities every 0.01 ps and running the *gmx tcaf* program to obtain the viscosity as a function of k vectors, and fitting to $\eta(k) = \eta(0)(1 - ak^2)$, were $\eta(0)$ is the kinematic viscosity extrapolating to k=0. Ninety-time samples of 10 ps length each were used to obtain ninety values of $\eta(0)$, these were averaged and the error bars were obtained from their standard deviations.

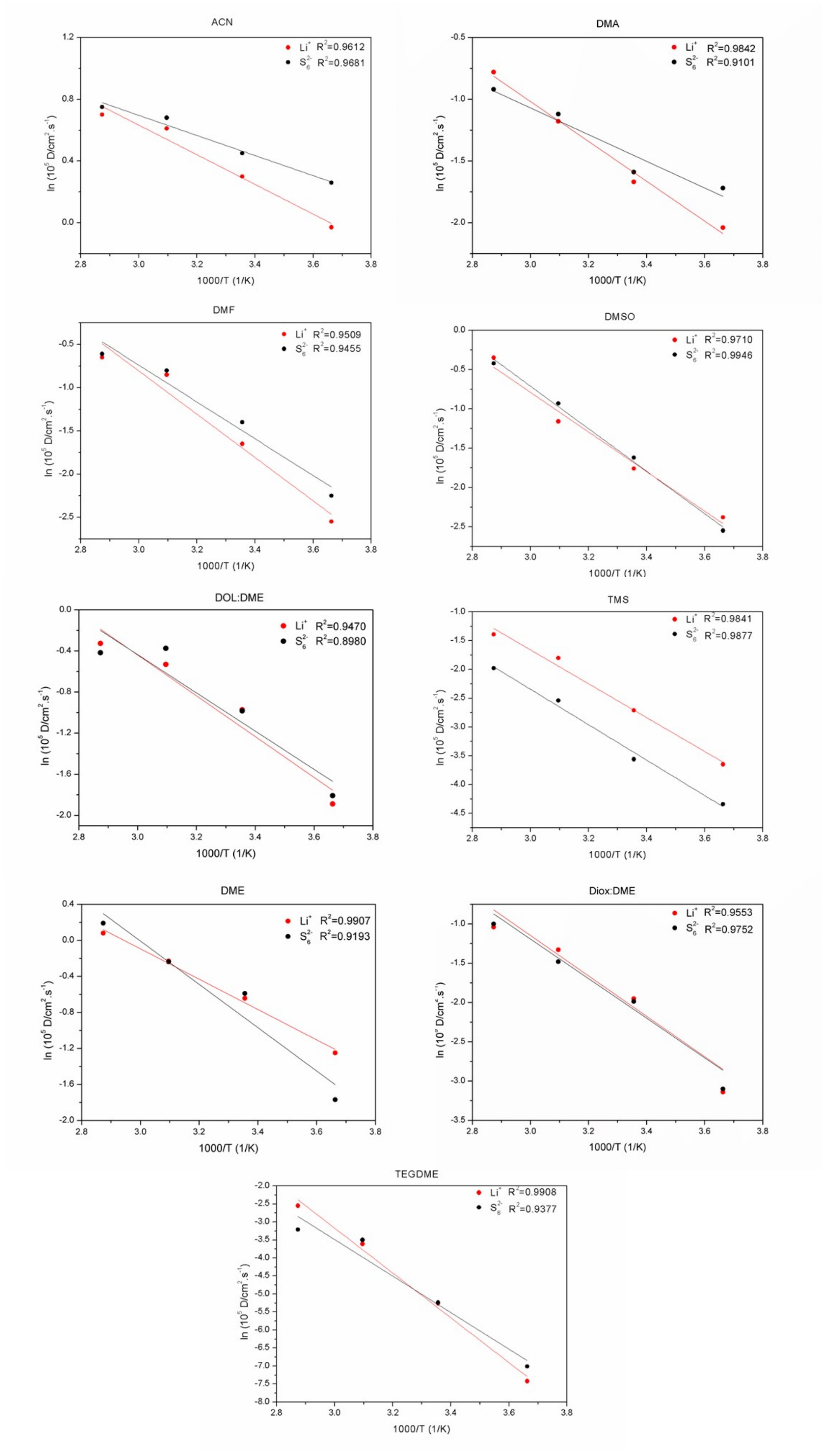

Figure S6. Arrhenius plots used to calculate the activation energy (E_a) for Li^+ diffusion.

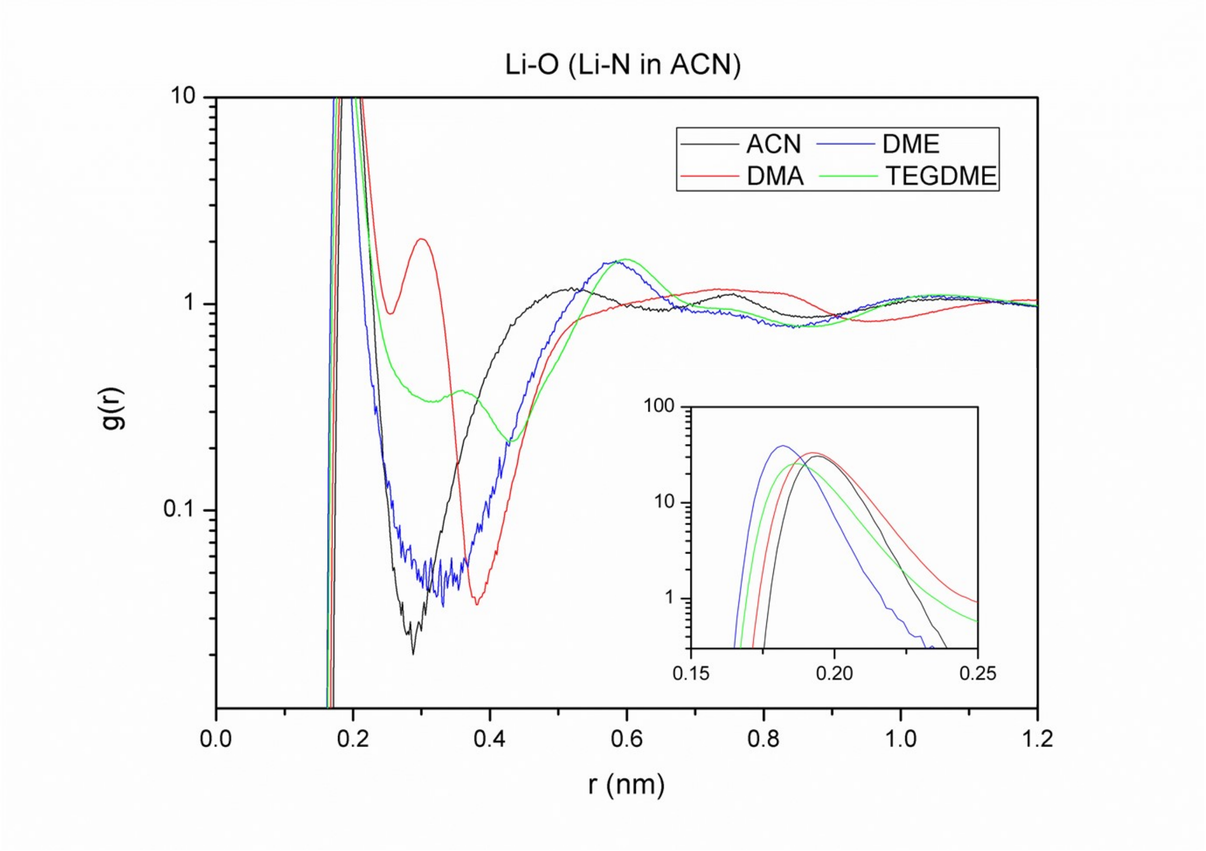

Figure S7. Radial distribution function (RDF) of the Li-O pair for the solvents DMA, DME and TEGDME (Li-N pair in the case of ACN). The inset shows a magnification of the first peak. Note the logarithmic scale in g(r).

Table S5. Position of the RDF first peak and coordination number (CN), obtained as the numerical integration of g(r) up to 0.25 nm, representing the C.N. of Li-O for DME, DMA and TEGDME, and C.N. of Li-N for ACN.

Solvent	r_{peak} (nm)	C.N.
ACN	0.196	3.982
DMA	0.192	2.969 *
DME	0.182	4.059
TEGDME	0.186	4.563

* The fourth coordination site of Li^+ is compensated by the nitrogen atom of one DMA molecule, with g(r) of Li-N showing r_{peak} = 0.192 nm and C.N.= 0.943.

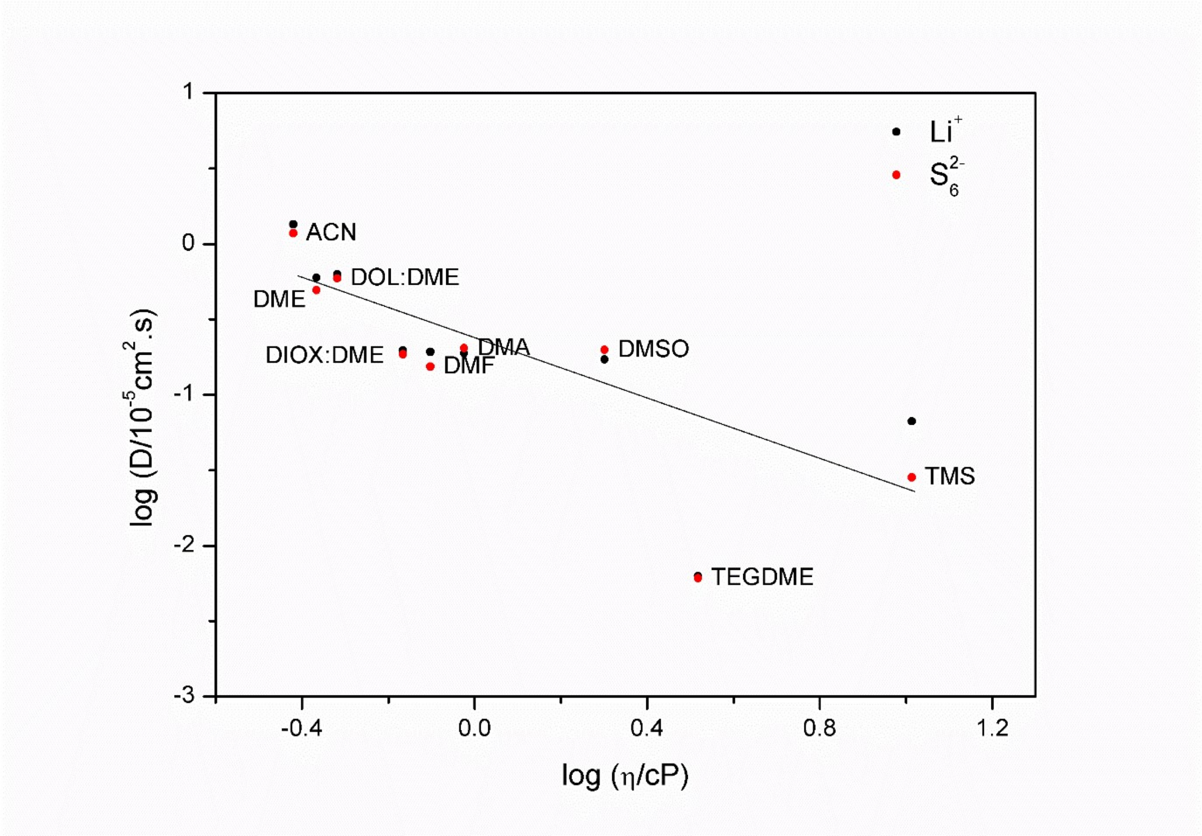

Figure S8. Plot of log (D) vs. log (η), the line has a slope $=-1$ to highlight the linear relationship $1/\mathrm{D}$ vs. η.

They were calculated by running 100 ps from the last frame obtained from the 100 ns simulations, saving velocities every 0.01 ps and running the *gmx tcaf* program to obtain the viscosity as a function of k vectors, and fitting to eta(k)=eta(0)*[1-a*k^2], were eta(0) is the kinematic viscosity extrapolating to k=0. Ninety time samples of 10 ps of length were used to obtain ninety values of eta(0), these were averaged and the error bars were obtained from their standard deviation.

MD Force Field validation

Validation studies by developers of the force-field

The force field parameterization has been reported in two publications, the first devoted to the electrolyte itself without polysulfides[3], whereas the second paper extends to polysulfides species Li_2S_8, Li_2S_6, Li_2S_4, Li_2S_2[5]. In particular, the first article[3] focuses on testing available force fields, computing the dielectric constant and viscosity of pure DOL, pure DME and DOL:DME mixtures, as well as adding LiTFSI supporting salt at various concentrations. The best match of force-field parameters was with those of Li^+ by Dang[9], and those of OPLS for DOL and DME solvent molecules. In particular, for the DME molecule the Anderson dihedral parameters[10] were adopted by Park et al.; however, in this study, we choose to adopt the original OPLS parameters for DME to be consistent with the other solvents studied herein.

The second article[5] focuses on the effect of different lithium polysulfides at various LiPS concentrations, the computation of ionic conductivity as well as clustering analysis, since it is well known that lower chain PS is less soluble and can be aggregated in clusters. The polysulfide parameters were taken from Rajput et al.[11], where sulfur atoms are modelled with DREIDING Lennard-Jones parameters and the S-S-S-S dihedral term is fitted to ab initio calculations. In particular, for the mixed sigma Li-S parameter, different Lennard-Jones parameters were tested by Park et al. coming from DREIDING, OPLS and CHARMM: a value of 0.275 nm was scaled from conductivity values calculated at various Li_2S_4 concentrations (see Figure S2 of reference[5]).

Comparison with DFT results from the literature

The enthalpies of solvation (with many solvent molecules) calculated according to the methodology described in the main article were compared with first-principles calculations from the literature[12], where only one solvent molecule is considered in interaction with a lithium polysulfide. This correlation is shown in Figure S9 below. Although the approaches are very different, we can see that they are roughly linearly correlated.

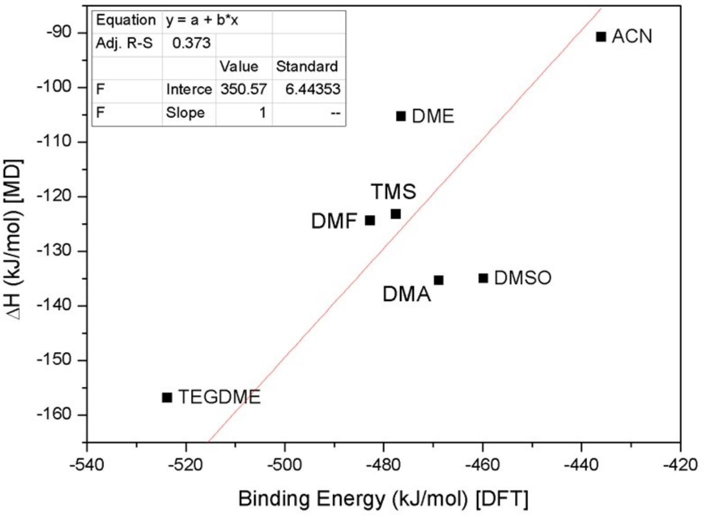

Figure S9. Plot of the computed ΔH trough MD simulations versus the Binding Energy of Li_2S_8 with one solvent molecule calculated by Density Functional Theory (DFT)[12] (see also https://rashatwi.github.io/combat/plots/be.html). The DFT calculations were performed in Gaussian using B3LYP exchange correlation functional with basis set 6-31+G* with D3 version of Grimme to account for dispersion terms.

In addition, we have computed the Li_2S_6 binding energy using the MD force field parameters with one solvent molecule:

$$E_{b,MD} = E_{Li_2S_6-solvent} - (E_{Li_2S_6} + E_{solvent})$$

In the right-hand side (RHS) of the equation, the first term is the energy of Li_2S_6 interacting with one solvent molecule inside a 3D pbc cubic box 10nm length, NVT 10 ps 200K, taking the lowest energy frame, and then subjected to energy minimization by conjugated gradients, convergence 1 kJ/mol. The second term of the RHS between parenthesis is the minimized energy by conjugated gradients of the Li_2S_6 centre of mass (c.o.m.) placed at (5, 5, 5), and the solvent molecule c.o.m. placed at (0, 0, 0) inside a 3D pbc cubic box 10nm length (non-interacting system). The computed values are matched against the binding energies computed through ab initio calculations reported in literature. The linear fit forced to pass through (0, 0) yields a good linear correlation as shown in Figure S10.

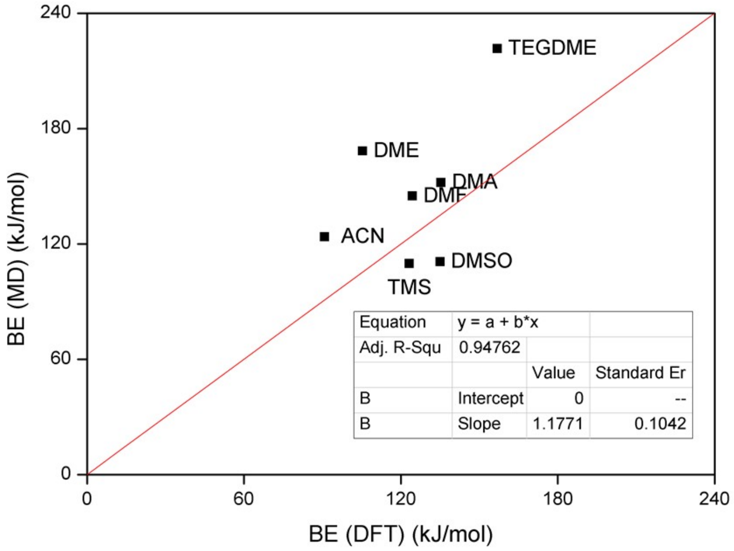

Figure S10. Comparison between Binding Energy (BE, absolute values) of Li_2S_6 computed with the MD force field of refs.[3,5] and the DFT values of ref.[12] referred to Li_2S_8.

Table S6. Solvation free energies of Li^+ computed using the procedure detailed in the manuscript, compared with experimental values for some of the solvents. The fourth column is the percentile difference between computed and experimental values. Composition of the systems were 1 Li^+ and the same number of solvent molecules as reported in Table S4.

	ΔG (kJ/mol)		
Solvent	Computed	Experimental(1)	C/E %diff.

ACN	-540.2	-460.7	17.3
DIOX-DME	-490.9		
DME	-525.3	-429.3	22.4
DMF	-486.9	-511.3	-4.8
DMSO	-561.3	-506.3	10.9
DOL-DME	-439.4		
TEGDME	-546.3		
TMS	-541.6	-482.8	12.2
DMA	-496.6	-510.9	-2.8

(1) Reference[13]

References

(1) Gutmann, V. The Extension of the Donor-Acceptor Concept. *Pure and Applied Chemistry* **1979**, *51* (11), 2197–2210. https://doi.org/10.1351/pac197951112197.

(2) Reis, J. C. R.; Lampreia, I. M. S.; Santos, Â. F. S.; Moita, M. L. C. J.; Douhéret, G. Refractive Index of Liquid Mixtures: Theory and Experiment. *ChemPhysChem* **2010**, *11* (17), 3722–3733. https://doi.org/10.1002/cphc.201000566.

(3) Park, C.; Kanduč, M.; Chudoba, R.; Ronneburg, A.; Risse, S.; Ballauff, M.; Dzubiella, J. Molecular Simulations of Electrolyte Structure and Dynamics in Lithium–Sulfur Battery Solvents. *Journal of Power Sources* **2018**, *373*, 70–78. https://doi.org/10.1016/j.jpowsour.2017.10.081.

(4) Fort, R. J.; Moore, W. R. Viscosities of Binary Liquid Mixtures. *Trans. Faraday Soc.* **1966**, *62*, 1112. https://doi.org/10.1039/tf9666201112.

(5) Park, C.; Ronneburg, A.; Risse, S.; Ballauff, M.; Kanduč, M.; Dzubiella, J. Structural and Transport Properties of Li/S Battery Electrolytes: Role of the Polysulfide Species. *J. Phys. Chem. C* **2019**, *123* (16), 10167–10177. https://doi.org/10.1021/acs.jpcc.8b10175.

(6) Abraham, M. J.; Murtola, T.; Schulz, R.; Páll, S.; Smith, J. C.; Hess, B.; Lindahl, E. GROMACS: High Performance Molecular Simulations through Multi-Level Parallelism from Laptops to Supercomputers. *SoftwareX* **2015**, *1–2*, 19–25. https://doi.org/10.1016/j.softx.2015.06.001.

(7) Luque Di Salvo, J.; Luque, G. L.; De Luca, G. Lithium Polysulfide Conformer Analysis in Ether-Based Solvents for Li–S Batteries. *Mol. Syst. Des. Eng.* **2022**, *7* (4), 364–373. https://doi.org/10.1039/D1ME00185J.

(8) Hess, B. Determining the Shear Viscosity of Model Liquids from Molecular Dynamics Simulations. *Journal of Chemical Physics* **2002**, *116*, 209–217. https://doi.org/10.1063/1.1421362.

(9) Dang, L. X. Development of Nonadditive Intermolecular Potentials Using Molecular Dynamics: Solvation of Li+ and F− Ions in Polarizable Water. *The Journal of Chemical Physics* **1992**, *96* (9), 6970–6977. https://doi.org/10.1063/1.462555.

(10) Anderson, P. M.; Wilson *, M. R. Developing a Force Field for Simulation of Poly(Ethylene Oxide) Based upon *Ab Initio* Calculations of 1,2-Dimethoxyethane. *Molecular Physics* **2005**, *103* (1), 89–97. https://doi.org/10.1080/00268970412331293811.

(11) Rajput, N. N.; Murugesan, V.; Shin, Y.; Han, K. S.; Lau, K. C.; Chen, J.; Liu, J.; Curtiss, L. A.; Mueller, K. T.; Persson, K. A. Elucidating the Solvation Structure and Dynamics of Lithium Polysulfides Resulting from Competitive Salt and Solvent Interactions. *Chem. Mater.* **2017**, *29* (8), 3375–3379. https://doi.org/10.1021/acs.chemmater.7b00068.

(12) Atwi, R.; Rajput, N. N. Guiding Maps of Solvents for Lithium-Sulfur Batteries via a Computational Data-Driven Approach. *Patterns* **2023**, *4* (9), 100799. https://doi.org/10.1016/j.patter.2023.100799.

(13) Itkis, D. Ambiguities in Solvation Free Energies from Cluster-Continuum Quasichemical Theory: Lithium Cation in Protic and Aprotic Solvents. *Phys. Chem. Chem. Phys.* **2021**, *23*, 16077. https://doi.org/10.1039/d1cp01454d.

(14) Sinnaeve, D. The Stejskal–Tanner Equation Generalized for Any Gradient Shape—an Overview of Most Pulse Sequences Measuring Free Diffusion. *Concepts Magnetic Resonance* **2012**, *40A* (2), 39–65. https://doi.org/10.1002/cmr.a.21223.

(15) Zou, Q.; Lu, Y.-C. Solvent-Dictated Lithium Sulfur Redox Reactions: An Operando UV–Vis Spectroscopic Study. *J. Phys. Chem. Lett.* **2016**, *7* (8), 1518–1525. https://doi.org/10.1021/acs.jpclett.6b00228.